The next frontiers for magnetic monopole searches

O. Gould,[1] I. Ostrovskiy,[2, a] and A. Upreti[2]

[1]*University of Nottingham, Nottingham, UK*

[2]*Department of Physics and Astronomy, University of Alabama, Tuscaloosa, Alabama, USA*

(Dated: September 17, 2024)

Magnetic monopoles (MMs) are well-motivated hypothetical particles whose discovery would symmetrize Maxwell equations, explain quantization of electric charge, and probe the gauge structure of the unified theory. Recent models predict MMs with low masses, reinvigorating searches at colliders. However, most theories predict composite MMs, whose production in parton-parton collisions is expected to be suppressed. The Schwinger process, whereby MM pairs tunnel through the vacuum barrier in the presence of a strong magnetic field, is not subject to this limitation. Additionally, the Schwinger cross section can be calculated nonperturbatively. Together, these make it a golden channel for low-mass MM searches. We investigate the Schwinger production of MMs in heavy-ion collisions at future colliders, in collisions of cosmic rays with the atmosphere, and in decay of magnetic fields of cosmic origin. We find that a next-generation collider would provide the best sensitivity. At the same time, exploiting the infrastructure of industrial ore extraction and Antarctic ice drilling could advance the field at a faster timescale and with only a modest investment. We also propose deploying dedicated MM detectors in conjunction with cosmic ray observatories to directly investigate if the unexplained, highest energy cosmic rays are MMs. Together, the proposed efforts would define the field of MM searches in the next decades.

The magnetic monopole (MM) is a hypothetical particle that carries isolated magnetic charge. It was postulated to exist by Dirac to explain the apparent quantization of the electric charge [1]. Dirac calculated the fundamental magnetic charge, called Dirac charge, to be:

$$g_{\mathrm{D}} = \frac{e}{2\alpha} \simeq 68.5e, \qquad (1)$$

where e is the proton charge and α is the fine-structure constant.

Dirac MMs are elementary particles with no internal structure. In contrast, solutions with isolated magnetic charge that appear in all variants of grand unified theories (GUT) that incorporate electromagnetism [2, 3] are composite objects – a bound state of carriers of the unified and electroweak interactions and other particles [4, 5]. The mass of a Dirac MM is a free parameter, while GUT MMs have masses on the order of the GUT scale, i.e., $\sim 10^{13}$ TeV/c^2. However, in models with several stages of symmetry breaking the MM mass is decreased accordingly. Such MMs could be produced after the inflationary epoch and would not catalyze proton decay [6, 7], evading the astrophysical limits on this process. Notably, composite finite-energy MM solutions have recently been discovered in several beyond-the-standard-model field theories, with masses as low as $\sim 10^0$ TeV/c^2 [8–15]. Unlike singly charged Dirac MMs, the fundamental magnetic charge predicted by theories based on spontaneously broken gauge symmetries may be n times larger than the Dirac charge, where n is an integer that depends on the global structure of the underlying symmetry group [16, 17]. For example, in the trinification model, where the MM only carries the U(1) and not color magnetic charges, the fundamental magnetic charge is three units of Dirac charge [18]. In an-

other instance, the Cho-Mason MM carries two units of Dirac charge [8]. String theories also contain MMs with masses that depend on the string scale, potentially much smaller than the GUT scale [19].

The proliferation of models suggesting low MM masses spurred experimental searches at the LHC. In the last few years, searches for production of MMs in p-p collisions were performed there by ATLAS [20–23] and MoEDAL [24–29]. Predicting the rate and kinematics of MM production is difficult because MMs couple strongly to photons, and so perturbative quantum field theory does not apply, unless appropriate resummation schemes are used [30, 31]. Consequently, the leading-order cross section calculations for the assumed Drell-Yan or photon-fusion mechanisms, which are used by the searches, can only be treated as indicative, and the corresponding mass limits are only suited for relative comparisons between experiments. Additionally, the quoted searches concentrate on the production of point-like MMs. This is because the production of composite MMs is expected to be suppressed by a huge factor of $\mathrm{e}^{-4/\alpha}$ in collisions of elementary particles [32, 33] due to negligible overlap between the initial and final states. A recently proposed approach to search for MM production in collisions of cosmic rays (CRs) with the atmosphere [34] is subject to the same limitation.

A different production method that overcomes the above limitations is the electromagnetic dual of the Schwinger mechanism [35–37], which describes electron-positron pairs tunnelling through the vacuum barrier in the presence of strong electric fields. As was shown [38, 39], MMs could similarly be produced by short-lived strong magnetic fields created when relativistic heavy ions pass by each other. Importantly, the finite size of composite MMs only enhances the production

rate [39, 40], and the rate can be calculated nonperturbatively [40, 41]. Additionally, it was shown recently that MMs could have been produced via the Schwinger effect by cosmological magnetic fields in the early universe [42, 43]. The first experimental search for MMs produced by the Schwinger mechanism was carried out by MoEDAL in the ultraperipheral Pb-Pb collisions at the LHC, establishing mass limits up to 75 GeV/c^2 at 95% C.L. for 1-3 g_D MMs [44]. While the sensitivity of such searches will increase during the upcoming heavy-ion runs at the LHC, HL-LHC [45], and HE-LHC [46], our projections show that the probed MM masses are unlikely to exceed 200-300 GeV/c^2, which does not reach the range suggested by theoretical models. The projections, whose methodology is described in more details in Ref. [47], are based on full Monte Carlo (MC) simulation of the relevant physics, realistic detector geometry of a MoEDAL-like detector, and expected luminosity targets. The question we ask is how one could get to the motivated mass region in the next few decades, if it's at all possible.

The paper considers three potential frontiers for next-generation MM searches – collisions of CRs with the atmosphere, man-made heavy-ion collisions, and relics from primordial phase transitions. MMs predicted by the theories cited above most commonly carry magnetic charges from 1 to 3 Dirac units, so this investigation focuses on that range.

Low-mass MMs could be continuously created in the Earth's atmosphere when CRs pass by atmosphere nuclei. Figure 1 illustrates the concept. According to Ampère's law, enormous magnetic fields are generated briefly during such flybys, giving rise to the Schwinger production of MMs. The MMs would travel downwards and, depending on their initial momentum, lose all momentum in the atmosphere, or slam into the surface. In the former case, the Earth's magnetic field will start guiding them towards the poles, where they will eventually touch down. In what follows, we describe the approach to calculating the production rate and trajectories of such MMs.

The production cross section and center-of-mass kinematics are calculated following the formalism developed in Refs. [41, 48]. To be conservative, we use the smaller of the two cross section approximations described in the references. The electromagnetic fields, E and B, produced by each considered ion are computed by integrating the Liénard-Wiechert potentials over classical nuclear charge distributions inferred from elastic scattering [49–51]. Due to the boost from the center-of-mass to the Earth frames, the produced MMs would be highly relativistic (Lorentz factors, or γ, of up to 10^5) and propagate towards the surface. The flux of incoming CRs is calculated using the Global Spline Fit [52], a data-driven model that characterizes the flux and composition from 10 GeV to 10^{11} GeV. Protons are the most abundant component of the CRs but produce a magnetic field with small total volume
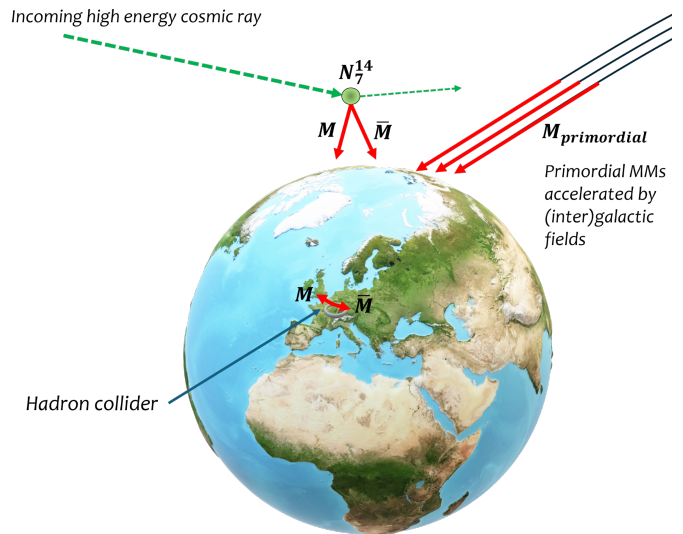

FIG. 1. Illustration of the three different MM sources considered in this work: a) MMs produced via the Schwinger process in ultraperipheral collisions of CRs with atmosphere nuclei; b) MMs produced via the Schwinger process in man-made heavy-ion collisions at a hadron collider; c) primordially produced MMs.

and energy, limiting the production of composite MMs. We quantify this threshold effect by ensuring that the energy density of the magnetic field integrated over its peak is greater than the energy of the monopole pair. Consequently, we concentrate on heavier components of CRs, which lead to larger magnetic field energies, in particular the iron ions. Similarly, while nitrogen is the most abundant element in the Earth's atmosphere, in some cases the interaction of CRs with heavier atmospheric elements such as oxygen, argon, or xenon results in higher production rates. The Schwinger production cross section calculated for relevant pairs of colliding ions, MM magnetic charge, and incoming CR energy is then compared to the Standard Model (SM) inelastic cross section (Figure 2). The latter accounts for competing processes that could destroy the CR before it produces a MM. We employ a toy MC to evaluate the fraction of such cases. The mean free paths for both interactions used in the random draws depend on the elevation. The atmosphere is approximated by a series of one hundred layers with different average densities and composition, from the surface up to the Kármán line, that are modeled according to the NRLMSISE standard atmospheric model [53]. We find that for all relevant MM masses and initial energies, no more than 1 in $\sim 10^5$ CR ions will produce a MM before experiencing an inelastic process. This estimate conservatively ignores MM production from secondaries, which could yield a few times more MMs, given that the highest fragmentation branching ratios for heavy nuclei
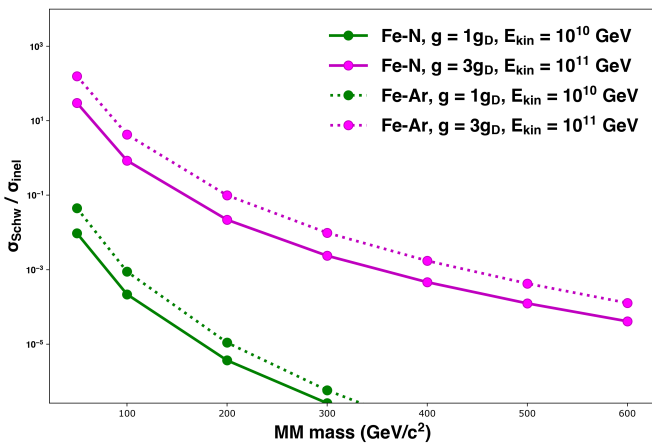
FIG. 2. The ratio of Schwinger MM production and inelastic scattering cross sections as a function of MM mass. Solid lines correspond to collision of CR iron ions with atmospheric nitrogen, while dash lines correspond to Fe-Ar collisions. Green lines correspond to initial CR energy of 10^{10} GeV and MM with 1 Dirac charge. Magenta lines correspond to CR energy of 10^{11} GeV and MMs with 3 units of Dirac charge.

with A nucleons are to $A - 1$ or $A - 2$ [54]. Evaluating possible experimental searches detailed later, we find that this channel is only sensitive to MMs with masses $\lesssim 80$ GeV/c² which are already excluded [44, 55]. It is worth emphasizing that this conclusion contradicts the claim that CR-atmosphere collisions set leading limits on 1-100 TeV/c² MM [34] because the latter work is not applicable to composite MMs, which are the type predicted by most modern models.

The next considered frontier is the man-made collisions. Currently, two similar proposals exist for the next-generation hadron collider, the FCC-hh [56] and SPPC [57]. The former is foreseen as a 100 TeV machine tentatively expected to start 40-45 years from now [58]. The latter is expected to reach 125 TeV and begin construction in at least 20 years [59]. Figure 3 shows projected sensitivity to MMs produced in Pb-Pb collisions via the Schwinger effect at the next collider. The calculation assumes the ultimate scenario [56] for the integrated luminosity of Pb-Pb collisions (110 nb^{-1}) for both the FCC-hh and SPPC machines and follows the same methodology as in Ref. [47]. Additionally, we anticipate progress in the detector technology and assume that future general-purpose collider detectors will be able to overcome the difficulties with reliable detection and reconstruction of highly ionizing particles [60], allowing them to combine their high efficiency (assumed 50% here [61]) with sensitivity to magnetic charges higher than 1 g_D. As the Figure shows, a 100-125 TeV machine will reach sensitivity to TeV/c² MM masses, addressing some of the existing models.

With the next-generation collider several decades away, we turn our attention to the third frontier – search
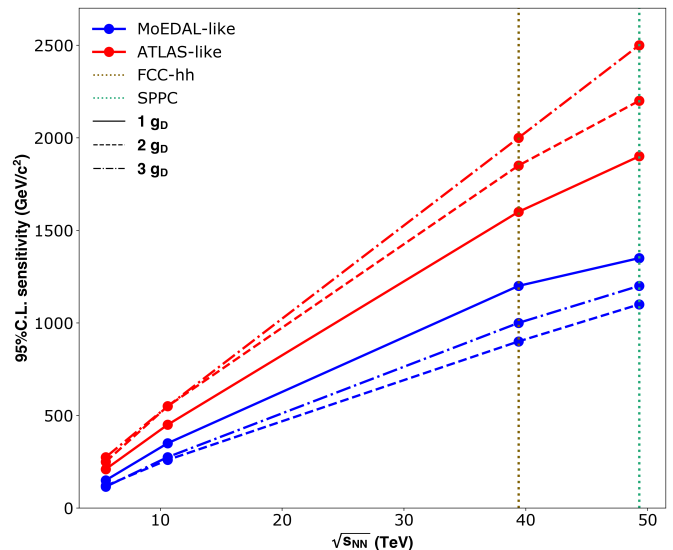

FIG. 3. Expected sensitivity of MM searches in Pb-Pb collisions as the function of the collision energy. The expected energies for the FCC-hh and SPPC machines are marked by the brown and jade dashed vertical lines, respectively. The blue lines correspond to a MoEDAL-like detector (location farther away from the interaction point, low efficiency), while the red dot-dashed line corresponds to a general-purpose like detector (location close to the interaction point, high efficiency) that is optimistically assumed to have zero background and able to detect multiply charged MMs.

for primordial MMs arriving to Earth as high-energy CRs. MMs predicted in theories based on broken symmetries are expected to have been produced in the early universe when the temperature was on the order of the relevant phase transition. The freeze-in of long-wavelength fluctuations through the transition is predicted to produce a finite density of MMs [62–65], which then do not annihilate efficiently [66]. For the case of heavy, GUT-scale MMs this created the so-called MM problem. However, this conclusion depends on relatively unconstrained early universe cosmology, including inflation and reheating. Crucially, if the reheating temperature is lower than the phase transition temperature, then MMs would not be formed this way. The reheating temperature could be as low as a few MeV, yielding weak constraints on MMs [67]. More recently, it has been realized that another potential source of cosmic MMs is the Schwinger process in primordial magnetic fields [42, 43]. Both low-mass and heavy MMs could have been produced by the Schwinger process in the early universe, but this mode of production also suffers from uncertainties, as the properties of the primordial fields are currently not well understood. Consequently, the disadvantage of all searches for primordial MMs is the inability to conclusively exclude the existence of MMs with a given mass, charge in case of a null result. Nevertheless, the possibility of a discovery motivates these searches, especially if existing

infrastructure could be exploited to minimize costs. In what follows, we propose three experimental directions and quantify their reach. Using detailed simulations and calculations, we demonstrate that the proposed searches are feasible and will lead to world-leading sensitivities to low-mass MMs during the next few decades. We choose the two staple detection methods that are optimized for detecting magnetic charge – NTDs and SQUID. The former are inexpensive, allow covering of large areas while having practically zero SM backgrounds [4]. A stack of NTDs can also allow differentiating between electric and magnetic charges by registering an increase or decrease of ionization density in subsequent layers. The latter method is the most direct and reliable way to identify an isolated magnetic pole bound to baryonic matter [68–74].

We assume that the flux of MMs produced in the early universe would be isotropic. Given the estimated strength and coherence lengths of (inter-)galactic magnetic fields, MMs lighter than $\lesssim 10^7$ TeV/c^2 would not be gravitationally bound to the galaxy and acquire relativistic velocities. A recent investigation allows for a wide range of γs of 1 g_D MMs passing by the Earth [75]. To calculate the sensitivity of a given experiment to primordially produced MMs, we first simulate incoming MMs with a given mass, charge, and Lorentz factor when entering the Earth's atmosphere ($\gamma_{\rm in}$). The MM physics, transportation, and energy losses are implemented using the Geant4 toolkit [76]. The MM's ionization energy losses are modeled using the formalism described in Refs. [77–79] that provide an accurate description of total energy loss from non-relativistic (down to β of 10^{-3}) to highly relativistic (γ up to 10^2) MMs. Pair production and bremsstrahlung are implemented as described in Ref. [80] and begin to dominate energy losses at higher energies (see Figure 4), with bremsstrahlung being the largest contributor for the MM masses considered here. Not included is the contribution from the photonuclear effect that competes with pair production at Lorentz factors above 10^4 but only weakly affects the results. The simulation geometry includes the Earth's surface, atmosphere, and an approximate description of the considered experiment. The atmosphere is simulated as described earlier. The Geant4 implementation of the Earth's magnetic field, crucial to simulate the trajectories of low-mass MMs, is based on the MAGNETOCOS-MICS model [81]. The model includes both the International Geomagnetic Reference Field (IGRF) [82] and external magnetospheric field [83]. The latter describes the field's asymmetry due to the solar wind.

The first experiment would take advantage of infrastructure developed at the south pole. As our simulations show, MMs with low $\gamma_{\rm in}$ would slow down in the atmosphere and be guided by the Earth's magnetic field towards the magnetic poles (also known as "dip" poles), producing an overabundance of touchdowns in these two areas, making them a natural locus for future searches.
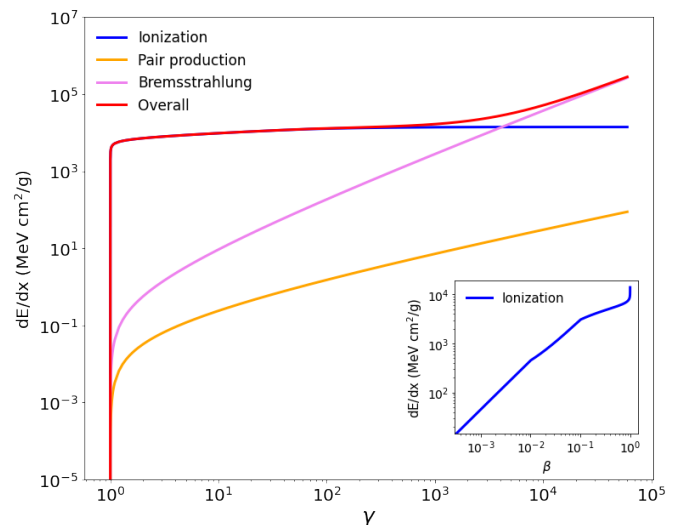

FIG. 4. Energy loss of a 100 GeV/c^2, 1 g_D MM in the atmosphere as a function of its Lorentz factor γ, as implemented in Geant4 simulation used in this work. The insert shows the energy loss of slow-moving MMs versus the MM's β, dominated by ionization (blue). Pair production (yellow) and bremsstrahlung (pink) begin to dominate the total energy loss (red) for Lorentz factors above $\sim 10^3$.

Figure 5 shows the increase in the rate of touchdowns near the magnetic poles predicted by the simulation for the low-mass MMs with $\gamma_{\rm in}$ of 1 to 1000, depending on the mass. While the exact location of the Earth's mag-
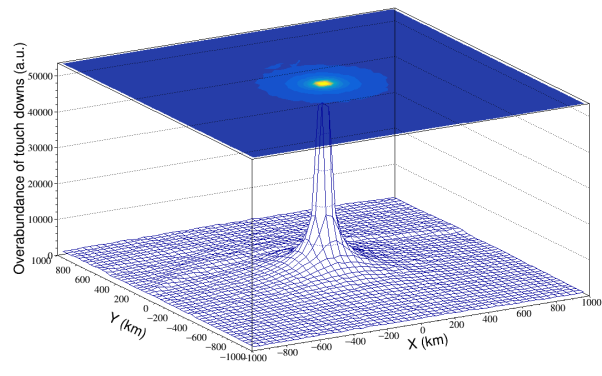

FIG. 5. The relative surface density of MMs touching down near the Earth's magnetic poles vs. the distance from the poles. The density spikes in the vicinity of the poles for MMs slow enough to be picked up by the Earth's magnetic field.

netic poles is subject to the geomagnetic secular variation, it coincides with the Earth's geographic poles when averaged over a few thousand years [84]. Upon hitting the surface, the MMs will quickly lose the remaining kinetic energy and get trapped by protons of the ice with a binding energy of 15-1000 keV [69]. The ice could then be

analyzed by a SQUID magnetometer for an unambiguous signature of an isolated magnetic charge – the persistent current. The South Pole Ice Core (SPICEcore) project drilled a 1751 m deep core in the ice near the geographic pole [85]. At its maximum depth, the SPICEcore samples date back $\sim$54k years [86]. During that period, the Earth's magnetic field varied considerably [87]. In particular, the polarity of the field reversed briefly (for a few hundred years) during the Laschamp excursion roughly 42k years ago. The polarity of the Earth's field does not affect the accumulation of MMs, since they are always created in pairs of opposite polarity. It is estimated that the average virtual axial dipole moment was 10-20% higher 50k years ago than now, before decreasing by a factor of two 40k years ago, then recovering to the peak value two thousands years ago, and finally decreasing again by 10-20% to the present value. The magnitude of the Earth's field affects the fraction of MMs that are picked up by the field. However, due to a large disparity between the initial kinetic energy of a MM and the potential energy of the Earth's magnetic field, a factor of two difference in the strength of the latter translates to just several tens of meters of the deceleration path in the atmosphere, so does not affect the results appreciably. The SPICEcore samples are 98 mm in diameter and up to 2 m in length, thus are small enough to pass through SQUID magnetometers used for MM searches [88]. The National Science Foundation Ice Core Facility (NSF-ICF) currently stores 13.2 cubic meters of ice from the drilling activity [89]. Scanning the existing samples could be accomplished in about a year. The exact flux limit depends on the value of the overabundance of touchdowns at the drilling location averaged over the age of the samples, which is difficult to calculate accurately. Here, we assume an overabundance that is two orders of magnitude lower than the maximum overabundance corresponding to the exact location of a dip pole, giving the 95% C.L. flux limit of approx. $<5 \cdot 10^{-22}$ cm^{-2}s^{-1}sr^{-1} for 1-3 g_D MMs with masses from 0.1 to up to a 100 TeV/c^2. This flux limit, shown in Figure 6, is substantially below the recently updated (seed-)galactic Parker bounds [75]. It is stronger than limits from other experiments [90, 91] but only applies to MMs with γ_{in} not exceeding the value of 1 to 1000, depending on the MM's mass. The experiment could be organized quickly, only requires a modest investment, and uses a detection technique that produces an unambiguous, background-free signature of magnetic charge. Other polar ice projects could also be included if possible. Notably, the Vostok ice core project has accumulated $\sim$40 m^3 of samples [92]. While less sensitive due to being extracted farther away from the geographic pole, these samples are interesting due to dating as far back as 420k years, so averaging over several cycles of the Earth's magnetic field variation. Finally, an experiment could extract small ice core samples from the exact historical locations of the geomagnetic south pole.
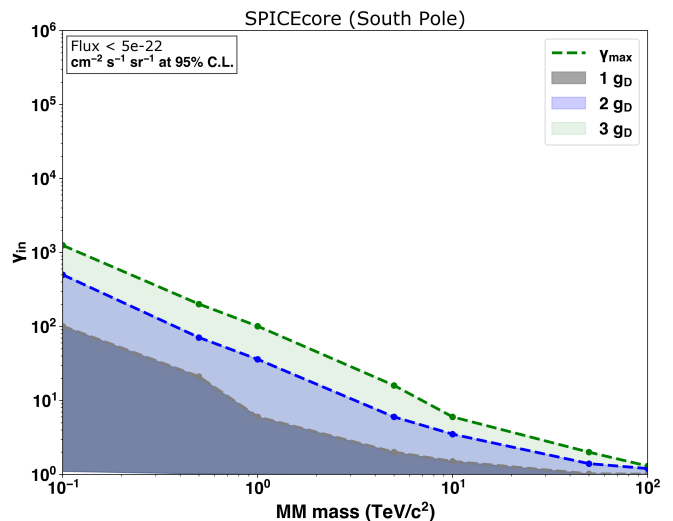

FIG. 6. Expected 95% C.L. exclusion limits on the flux of cosmic MMs if none are found to be trapped in the SPICEcore samples. Fluxes of MMs with masses and initial Lorentz factors in the shaded regions are excluded. Grey, indigo, and green lines correspond to MMs with 1, 2, and 3 units of Dirac charge, respectively. The dashed lines show the boundaries of the max initial Lorentz factors.

The locations are known by direct measurements since 1909 and remain on-shore until early 1960s. The samples need to be extracted from only a couple of meters depth. While each sample would correspond to roughly one year exposure, the overabundance of touchdowns for MMs for small γ_{in} would be equivalent to more than 10^4 yrs of accumulation at a location far away from the dip poles.

Another approach is deploying a much larger array of NTDs than was used by previous experiments. Similar proposals were made earlier [93, 94], aiming to place the array on a mountain substantially above the sea level to improve sensitivity to low masses and γ_{in}. Since such a placement is challenging and expensive, we first consider a ground-level NTD array, with an 50000 m^2 coverage area, comparable to the cited proposals. Assuming a 10-year exposure, the expected 95% C.L. flux limit is $<3.0 \cdot 10^{-18}$ cm^{-2}s^{-1}sr^{-1} for 1-3 g_D MMs with masses from 0.1 to up to a 100 TeV/c^2. Complementary to the SPICEcore proposal, the limit for this frugal and more realistic option applies to a region of γ_{in} *exceeding* values of $\sim 10^0$ to $\sim 10^3$, depending on the mass (Figure 7). It surpasses current experiments [90, 91] for $\log_{10}(\gamma_{in})$ less than 7–9, depending on the mass. An NTD array can also cover the full region of Lorentz factors and masses if placed as close to the present location of the Earth's magnetic pole as practical. It would additionally collect the contribution from MMs that slowed down in the atmosphere and were transported by the Earth's magnetic field. This addition, like with the SPICEcore, would im-
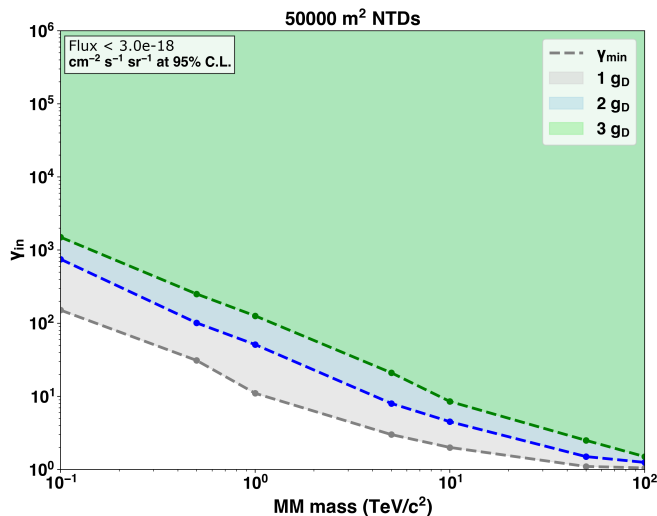
FIG. 7. Expected 95% C.L. exclusion limits on the flux of cosmic MMs if none are detected by the 50k m² NTD array after a 10-year exposure. Fluxes of MMs with masses and initial Lorentz factors in the shaded regions are excluded. Grey, indigo, and green lines correspond to MMs with 1, 2, and 3 units of Dirac charge, respectively. The dashed lines show the boundaries of the minimum initial Lorentz factors.

prove sensitivity to MMs with low masses and $\gamma_{\rm in}$. The closest permanent stations that could provide support (in order of increasing distance from the current location of the south magnetic pole) are the French's Dumont d'Urville Station, Russian's Vostok Station, and the U.S. South Pole Station, the latter two located at the geomagnetic and geographic south poles, respectively. Both the lower-energy MMs guided by the Earth's magnetic field and higher-energy ones that impact directly above the deployment would pass through several layers of NTDs, producing a characteristic signature. The antarctic placement still suffers from being remote and associated high costs but is perhaps more advantageous than the mountain alternative. The flux limit for the region of small $\gamma_{\rm in}$ is estimated to be $<2.0 \cdot 10^{-23}$ cm^{-2}s^{-1}sr^{-1} for 1-3 $g_{\rm D}$ MMs with masses from 0.1 to up to a 100 TeV/c². In case of a candidate event, the material below the specific NTD stack could be investigated for the presence of a stopped, bound MM using a magnetometer. While NTDs are inexpensive, a big challenge with all proposed large-area NTD deployments is the time and cost needed to chemically etch, scan, and analyze such large areas. A promising way to alleviate this is by adding layer(s) of dedicated electronic detectors that are, like the NTDs, inexpensive and sensitive only to highly ionizing particles [95]. Segmented in a way similar to the NTD sheets, they could pinpoint the location of candidate events, drastically reducing the NTD area that needs to be processed. The analysis step could be further sped up by emerging machine learning techniques [96].

An important potential placement for an array of NTDs is at a cosmic ray observatory, such as the Pierre Auger Observatory, Large High Altitude Air Shower Observatory, or Telescope Array Project. Some of the detected ultra-high energy cosmic rays (UHECRs), defined as CRs with an energy greater than 1 EeV, do not have trajectories pointing back to any plausible astrophysical sources [97] and have energies larger than what could be explained by the known acceleration mechanisms and what is possible for known particles of remote, intergalactic origin [98–100]. It has long been suggested that UHECRs are primordial low-mass MMs [101] because they are expected to be accelerated to similarly large energies by the intergalactic and galactic magnetic fields and have trajectories not pointing back to specific sources. The recent detection of the Amaterasu particle [97] has reinvigorated such discussions [102, 103]. While the Pierre Auger Observatory has published a MM search [91], the experiment is not directly sensitive to magnetic charge and relies on understanding of the MM's air shower profile, which is subject to model-dependent uncertainties. In contrast, placing large arrays of NTDs or other detectors that are reliably sensitive to magnetic charge on the territory of a cosmic ray observatory could directly check the hypothesis of the MM origin of UHECRs. An UHECR's shower core can be located by the observatory with a 50 m resolution [104], corresponding to the ground area of $\sim$8000 m². A 50000 m² NTD array would then be sufficient to provide a coincidence measurement, with the UHECRs' reconstructed position serving as a definitive trigger for the NTD scan. Such an array would only cover a small fraction of the total surface area monitored by the observatory. However, given the measured flux of UHECRs [105], the expected rate of UHECRs with >4 EeV detected in coincidence with the NTD array would be 1 every 5 to 6 years.

Lastly, we consider bringing the earlier searches for MMs trapped in the Earth-based rocks [106] and deep sea sediments [107, 108] to the next level by exploiting industrial capabilities. Slowed-down MMs are expected to bind to iron and aluminum nuclei with large binding energies [69, 70]. The production of these metals is currently performed on a vast scale, with $\sim$1M tons of raw ore processed by some facilities every year. In a typical factory, crushed ore is transported by one or more conveyors at speeds of up to several meters per second for up to 5k annual operating hours each year [109]. The operating company may allow installing a bypass equipped with one or more SQUID magnetometers through which just a small fraction of the total ore would pass, perhaps motivated by publicity and outreach considerations. To estimate the sensitivity of this approach, we consider one concrete example. The iron ore deposits at the Carajas-Serra Norte mine in Vale, Brazil, are ca. 1590 Mtons [110] of grade higher than 64% Fe and estimated exposure time of 2.7G years [111]. Based on our calculations, processing of 1k tons of iron ore per year (just $\sim$0.001% of total processed

by the company) for one year will result in 95% C.L. flux limits of $<5.5\cdot10^{-22}$ cm^{-2}s^{-1}sr^{-1} for 1-3 g_D MMs. The limits, shown on Figure 8, are extremely strong but apply to the specific range of γ_{in}, dictated by the location of the deposits and MMs' energy losses. Other mines, e.g., the Weipa bauxite mine, Mount Whaleback, and Sischen iron ore mines, would provide similar sensitivity for different ranges of γ_{in} depending on the depth of the deposits.
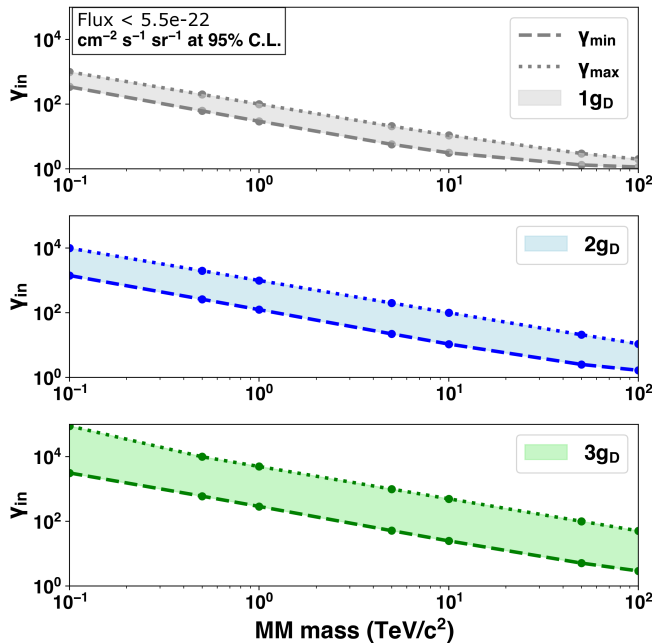

FIG. 8. Exclusion limits on cosmic MM flux as a function of mass and initial Lorentz factor. The limits correspond to a null result of scanning 1k tons of iron ore deposits in Vale, Brazil. The shaded regions are excluded. The dashed (dotted) lines show the boundaries of the min (max) initial Lorentz factors. Grey, blue, and green colors corresponds to MMs with 1, 2, and 3 units of Dirac charge. Deposits of iron and aluminum ore in other locations could allow similar limits for different ranges of initial Lorentz factors, depending on the depth of the deposits.

To summarize, the proposed experiments would provide world-leading sensitivities to low-mass MMs until the next hadron collider turns on, two to four decades from now. While null results would not be as informative as that from a Schwinger production experiment at a collider, they offer the best chance of a discovery at a small fraction of the cost and effort, bringing the long-standing quest for isolated magnetic charge closer to completion.

This study has focused on the unique electromagnetic interactions of MMs. For composite MMs, there are model-dependent non-electromagnetic interactions which are typically limited to the region of the MM core, and which may yield additional signatures. The cross section calculation used in this work is also known to be conservative. Future development in this area is likely to strengthen the projections.

A key point is that this work goes beyond setting flux limits based on indirect observations by non-dedicated experiments. The MM production cross section for the Schwinger process is calculable nonperturbatively and is not subject to the exponential suppression for composite MMs, while the proposed primordial MM detection efforts are unambiguously sensitive to magnetic charge. Consequently, even a negative result of the proposed collider searches would reliably exclude the existence of MMs with specific masses and charges, while the results of cosmic searches, especially conducted in conjunction with the CR observatories, could confirm or refute the suggestion that UHECRs are MMs.

Author Contributions. Simulations, statistical analysis, results, and figures were produced by A. Upreti. Theoretical calculations of the Schwinger production rates were done by O. Gould who also helped edit the manuscript. I. Ostrovskiy conceived and supervised the project, wrote and edited the manuscript. All authors have read and agreed to the final version of the manuscript.

Data Availability Statement. Data supporting this study is available upon request. The code for computing the electromagnetic fields of ion pairs is available at [112]. The code for generating the sensitivity plots is available at [113].

[a] Corresponding author: iostrovskiy@ua.edu
[1] P. A. M. Dirac, Proc. R. Soc. Lond. **133**, 60 (1931).
[2] G. Hooft, Nucl. Phys. B **79**, 276 (1974).
[3] A. M. Polyakov, JETP Lett. **20**, 194 (1974).
[4] L. Patrizii and M. Spurio, Annu. Rev. Nucl. Part. Sci. **65**, 279 (2015).
[5] N. E. Mavromatos and V. A. Mitsou, Int. J. Mod. Phys. A **35**, 2030012 (2020).
[6] T. W. Kephart and Q. Shafi, Phys. Lett. B **520**, 313 (2001).
[7] K. Olive and P. D. Group, Chin. Phys. C **38**, 090001 (2014).
[8] Y. Cho and D. Maison, Phys. Lett. B **391**, 360 (1997).
[9] K. Kimm, J. H. Yoon, and Y. M. Cho, Eur. Phys. J. C **75**, 67 (2015).
[10] J. Ellis, N. E. Mavromatos, and T. You, Phys. Lett. B **756**, 29 (2016).
[11] N. E. Mavromatos and S. Sarkar, Phys. Rev. D **95**, 104025 (2017).
[12] S. Arunasalam and A. Kobakhidze, Eur. Phys. J. C **77**, 444 (2017).

[13] N. E. Mavromatos and S. Sarkar, Phys. Rev. D **97**, 125010 (2018).

[14] P. Q. Hung, Nucl. Phys. B **962**, 115278 (2021).

[15] F. Blaschke and P. Beneš, Prog. Theor. Exp. Phys. **2018**, 073B03 (2018).

[16] E. Corrigan and D. I. Olive, Nucl. Phys. B **110**, 237 (1976).

[17] D. Tong, JHEP **07**, 104 (2017).

[18] G. Lazarides and Q. Shafi, Phys. Lett. B **818**, 136363 (2021).

[19] X.-G. Wen and E. Witten, Nucl. Phys. B **261**, 651 (1985).

[20] G. Aad, T. Abajyan, B. Abbott, *et al.* (ATLAS Collaboration), Phys. Rev. Lett. **109**, 261803 (2012).

[21] G. Aad, B. Abbott, *et al.* (ATLAS Collaboration), Phys. Rev. D **93**, 052009 (2016).

[22] G. Aad *et al.* (ATLAS Collaboration), Phys. Rev. Lett. **124**, 031802 (2020).

[23] G. Aad *et al.* (ATLAS), JHEP **11**, 112 (2023).

[24] B. Acharya *et al.* (MoEDAL Collaboration), JHEP **08**, 067 (2016).

[25] B. Acharya *et al.* (MoEDAL Collaboration), Phys. Rev. Lett. **118**, 061801 (2017).

[26] B. Acharya *et al.* (MoEDAL Collaboration), Phys. Rev. Lett. **123**, 021802 (2019).

[27] B. Acharya *et al.* (MoEDAL Collaboration), Phys. Lett. B **782**, 510 (2018).

[28] B. Acharya *et al.* (MoEDAL Collaboration), Eur. Phys. J. C **82**, 694 (2022).

[29] B. Acharya *et al.* (MoEDAL Collaboration), (2023), arXiv:2311.06509 [hep-ex].

[30] J. Alexandre and N. E. Mavromatos, Phys. Rev. D **100**, 096005 (2019).

[31] S. Baines, N. E. Mavromatos, V. A. Mitsou, J. L. Pinfold, and A. Santra, Eur. Phys. J. C **78**, 966 (2018), [Erratum: Eur.Phys.J.C 79, 166 (2019)].

[32] E. Witten, Nucl. Phys. B **160**, 57 (1979).

[33] A. K. Drukier and S. Nussinov, Phys. Rev. Lett. **49**, 102 (1982).

[34] S. Iguro, R. Plestid, and V. Takhistov, Phys. Rev. Lett. **128**, 201101 (2022).

[35] J. Schwinger, Phys. Rev. **82**, 664 (1951).

[36] W. Heisenberg and H. Euler, Z. Phys. **98**, 714 (1936).

[37] F. Sauter, Z. Phys. **69**, 742 (1931).

[38] I. K. Affleck and N. S. Manton, Nucl. Phys. B **194**, 38 (1982).

[39] D. L. J. Ho and A. Rajantie, Phys. Rev. D **103**, 115033 (2021).

[40] D. L.-J. Ho and A. Rajantie, Phys. Rev. D **101**, 055003 (2020).

[41] O. Gould, D. L.-J. Ho, and A. Rajantie, Phys. Rev. D **100**, 015041 (2019).

[42] T. Kobayashi, Phys. Rev. D **104**, 043501 (2021).

[43] T. Kobayashi and D. Perri, Phys. Rev. D **106**, 063016 (2022).

[44] B. Acharya *et al.* (MoEDAL Collaboration), Nature **602**, 63 (2022).

[45] O. Brüning and L. Rossi, CERN Yellow Rep. Monogr. **10**, 1 (2020).

[46] A. Abada *et al.* (FCC), Eur. Phys. J. ST **228**, 1109 (2019).

[47] D. d'Enterria *et al.*, J. Phys. G **50**, 050501 (2023).

[48] O. Gould, D. L. J. Ho, and A. Rajantie, Phys. Rev. D **104**, 015033 (2021).

[49] H. De Vries, C. W. De Jager, and C. De Vries, Atom. Data Nucl. Data Tabl. **36**, 495 (1987).

[50] J. D. Lewin and P. F. Smith, Astropart. Phys. **6**, 87 (1996).

[51] Z.-F. Cui, D. Binosi, C. D. Roberts, and S. M. Schmidt, Phys. Rev. Lett. **127**, 092001 (2021).

[52] H. P. Dembinski, R. Engel, A. Fedynitch, T. Gaisser, F. Riehn, and T. Stanev, PoS **ICRC2017**, 533 (2018).

[53] J. T. Emmert *et al.*, Earth Space Sci. **8**, e2020EA001321 (2021).

[54] L. Morejon, A. Fedynitch, D. Boncioli, D. Biehl, and W. Winter, JCAP **11**, 007 (2019).

[55] B. Acharya *et al.* (MoEDAL Collaboration), Phys. Rev. Lett. **133**, 071803 (2024).

[56] A. Abada *et al.* (FCC), Eur. Phys. J. ST **228**, 755 (2019).

[57] W. Abdallah *et al.* (CEPC Study Group), (2023), arXiv:2312.14363 [physics.acc-ph].

[58] I. Agapov *et al.*, (2022), arXiv:2203.08310 [physics.acc-ph].

[59] J. Tang, Y. Zhang, Q. Xu, J. Gao, X. Lou, and Y. Wang, in *Snowmass 2021* (2022) arXiv:2203.07987 [hep-ex].

[60] M. Arslandok, H. Caines, and M. Ivanov, (2024), arXiv:2403.12299 [physics.ins-det].

[61] G. Aad *et al.* (ATLAS Collaboration), JHEP **11**, 112 (2023).

[62] T. W. B. Kibble, J. Phys. A **9**, 1387 (1976).

[63] W. H. Zurek, Nature **317**, 505 (1985).

[64] M. Hindmarsh and A. Rajantie, Phys. Rev. Lett. **85**, 4660 (2000).

[65] A. Rajantie, Phys. Rev. D **68**, 021301 (2003).

[66] Y. B. Zeldovich and M. Y. Khlopov, Phys. Lett. B **79**, 239 (1978).

[67] O. Gould and A. Rajantie, Phys. Rev. Lett. **119**, 241601 (2017).

[68] K. A. Milton *et al.*, Int. J. Mod. Phys. A **17**, 732 (2002).

[69] K. A. Milton, Rep. Prog. Phys. **69**, 1637 (2006).

[70] C. Kittel and A. Manoliu, Phys. Rev. B **15**, 333 (1977).

[71] C. Goebel, in Monopole '83, J.L. Stone ed., Plenum , 333 (1984).

[72] L. Gamberg, G. R. Kalbfleisch, and K. A. Milton, Found Phys **30**, 543 (2000).

[73] L. Bracci and G. Fiorentini, Nucl. Phys. B **232**, 236 (1984).

[74] K. Olaussen and R. Sollie, Nucl. Phys. B **255**, 465 (1985).

[75] D. Perri, K. Bondarenko, M. Doro, and T. Kobayashi, (2023), arXiv:2401.00560 [hep-ph].

[76] S. Agostinelli *et al.* (Geant4), Nucl. Instrum. Meth. A **506**, 250 (2003).

[77] S. P. Ahlen, Phys. Rev. **D17**, 229 (1978).

[78] S. Cecchini, L. Patrizii, Z. Sahnoun, G. Sirri, and V. Togo, (2016), arXiv:1606.01220 [physics.ins-det].

[79] S. p. Ahlen and K. Kinoshita, Phys. Rev. D **26**, 2347 (1982).

[80] S. D. Wick, T. W. Kephart, T. J. Weiler, and P. L. Biermann, Astropart. Phys. **18**, 663 (2003).

[81] L. Desorgher and others., Int. J. Mod. Phys. A **20**, 6802 – 6804 (2005).

[82] P. Alken *et al.*, Earth Planets Space **73**, 49 (2021).

[83] N. Tsyganenko, Planet. Space Sci. **37**, 5 (1989).

[84] in *The Magnetic Field of the Earth*, International Geophysics, Vol. 63, edited by R. T. Merrill, M. W. McEl-

hinny, and P. L. McFadden (Academic Press, 1998) pp. 217–263.

[85] J. A. Johnson *et al.*, Ann. Glaciol. **62**, 75–88 (2021).

[86] D. A. Winski *et al.*, Clim. Past **15**, 1793 (2019).

[87] C. Constable, "Dipole moment variation," in *Encyclopedia of Geomagnetism and Paleomagnetism*, edited by D. Gubbins and E. Herrero-Bervera (Springer Netherlands, Dordrecht, 2007) pp. 159–161.

[88] J. C. Schouten, A. D. Caplin, C. N. Guy, M. Hardiman, M. Koratzinos, and W. S. Steer, J. phys. E. **20**, 850 (1987).

[89] C. LaBombard, (2023), private communication.

[90] R. L. Workman *et al.* (Particle Data Group), PTEP **2022**, 083C01 (2022).

[91] A. Aab *et al.* (Pierre Auger), Phys. Rev. D **94**, 082002 (2016).

[92] J. R. Petit *et al.*, Nature **399**, 429 (1999).

[93] J. Pinfold, EPJ Web Conf. **145**, 12002 (2017).

[94] V. Mitsou (MoEDAL Collaboration), PoS **DISCRETE2020-2021**, 017 (2022).

[95] I. Ostrovskiy and J. Pinfold, (2014), arXiv:1410.5521 [physics.ins-det].

[96] A. J. Bevan, Phil. Trans. Roy. Soc. Lond. A **377**, 20190392 (2019).

[97] R. U. Abbasi *et al.* (Telescope Array), Science **382**, abo5095 (2023).

[98] G. T. Zatsepin and V. A. Kuzmin, JETP Lett. **4**, 78 (1966).

[99] K. Greisen, Phys. Rev. Lett. **16**, 748 (1966).

[100] F. W. Stecker, Phys. Rev. **180**, 1264 (1969).

[101] T. J. Weiler and T. W. Kephart, Nucl. Phys. B Proc. Suppl. **51**, 218 (1996).

[102] Y. M. Cho and F. H. Cho, Phys. Lett. B **851**, 138598 (2024).

[103] P. H. Frampton and T. W. Kephart, Phys. Lett. B **855**, 138777 (2024).

[104] M. Mostafa, Nucl. Phys. B Proc. Suppl. **165**, 50 (2007), arXiv:astro-ph/0608670.

[105] A. Aab *et al.* (Pierre Auger), Science **357**, 1266 (2017).

[106] K. Bendtz *et al.*, Phys. Rev. Lett. **110**, 121803 (2013).

[107] H. H. Kolm, F. Villa, and A. Odian, Phys. Rev. D **4**, 1285 (1971).

[108] R. L. Fleischer *et al.*, Phys. Rev. **184**, 1393 (1969).

[109] G. Thomas and P. Conley, in *Overland bauxite conveying – cable hauled conveyors vs. conventional conveyors* (JLV Industries Pty Ltd, 1999).

[110] Alessandro Resende at al., "Technical Report Summary - Serra Norte Complex," (2021), [December 31, 2021, minedocs.com].

[111] A. Trendall *et al.*, J South Am Earth Sci **11**, 265 (1998).

[112] O. Gould, "emions," `https://bitbucket.org/og113/emions/` (2024), v1.0.0.

[113] A. Upreti, "projbox," `https://cernbox.cern.ch/s/whoqoC81rLdvTjP` (2024), v1.0.0.